



Deposited via The University of Sheffield.

White Rose Research Online URL for this paper:

<https://eprints.whiterose.ac.uk/id/eprint/157776/>

Version: Accepted Version

---

**Article:**

Xu, H., Zhang, J., Liu, W. et al. (2020) High resolution radar waveform design based on target information maximization. *IEEE Transactions on Aerospace and Electronic Systems*, 56 (5). pp. 3577-3587. ISSN: 0018-9251

<https://doi.org/10.1109/taes.2020.2976085>

---

© 2020 IEEE. Personal use of this material is permitted. Permission from IEEE must be obtained for all other users, including reprinting/ republishing this material for advertising or promotional purposes, creating new collective works for resale or redistribution to servers or lists, or reuse of any copyrighted components of this work in other works. Reproduced in accordance with the publisher's self-archiving policy.

**Reuse**

Items deposited in White Rose Research Online are protected by copyright, with all rights reserved unless indicated otherwise. They may be downloaded and/or printed for private study, or other acts as permitted by national copyright laws. The publisher or other rights holders may allow further reproduction and re-use of the full text version. This is indicated by the licence information on the White Rose Research Online record for the item.

**Takedown**

If you consider content in White Rose Research Online to be in breach of UK law, please notify us by emailing [eprints@whiterose.ac.uk](mailto:eprints@whiterose.ac.uk) including the URL of the record and the reason for the withdrawal request.

# High Resolution Radar Waveform Design Based on Target Information Maximization

Huaping Xu, *Member, IEEE*, Jiawei Zhang, *Student Member, IEEE*, Wei Liu, *Senior Member, IEEE*,  
Shuang Wang, Chunsheng Li

**Abstract**—Although the transmit radar waveform design problem for maximizing target information has been studied widely in the past, the resolution requirement is normally ignored in such designs. Using maximizing target information as a criterion, a new radar waveform design method meeting the high resolution requirement is proposed in this paper, which makes no assumptions on the statistical distribution of target scattering. The objective function is proposed by maximizing the Pearson correlation coefficient (PCC) and the design is then transformed into an optimization problem, which is solved in two steps. Firstly, a closed-form expression for the discretized waveform with constant power constraint is derived in the time domain. Secondly, based on the bandwidth analysis of the optimal solution, a resolution improvement method considering information distortion is introduced and a suboptimal waveform is proposed while satisfying the constant power and resolution requirements. Finally, performance of the proposed radar waveform in terms of information acquisition, classification and resolution is analyzed and compared with the classic high-resolution linear frequency modulated waveform (LFMW). Simulation results show that the resolution of the suboptimal waveform is slightly lower than the LFMW, but more desirable in terms of peak sidelobe ratio (PSLR), information acquisition and classification.

**Index Terms**—Information acquisition, radar waveform design, high resolution, constrained optimization, distortion.

## I. INTRODUCTION

**R**ADAR design aims to maximize the acquisition of target information and thus achieve high-precision detection, classification and finally recognition [1-3]. Thanks to high-resolution imaging radar, such as synthetic aperture radar (SAR), even micro, small and closely spaced targets become visible and identifiable [3, 4]. The transmitted radar waveform determines range resolution, and it can be viewed as a channel for radar to acquire information. Therefore, how to design a better waveform to maximize the acquired information from targets and obtain high resolution as well, is of great significance.

As one of the classic waveforms and widely used in imaging radar [5-8], the linear frequency modulated waveform (LFMW) is optimal under the signal to noise ratio (SNR) maximization criterion for point targets, but it does not exhibit superior information acquisition capability, especially for extended or spatially spread targets [9].

As early as 1964, Woodward pointed out that pursuing SNR blindly can mislead radar design and data processing because there is no theory which implies that maximizing SNR can ensure maximal information acquirement [10]. A similar issue was also raised by Bell in [11]. Therefore, it would be important and also beneficial to develop some high resolution waveform design methods under the maximizing target information criterion (MTIC), so that higher amount of target information can be acquired for improving target perception performance.

In the past, the study of waveform design based on the MTIC was mainly focused on non-imaging radars without high resolution requirement, and these studies can be classified into three categories: single waveform radar, multi-input multi-output (MIMO) radar and cognitive radar. Woodward carried out a preliminary study by applying information theory to radar systems soon after the work of the classic information theory by Shannon [10]. Subsequently, Bell's seminal work in [12] explored the connection between information theoretic tools and waveform design. With the Gaussian assumption of the scattering signal and mutual information (MI) as an objective function, they provided a design method for the amplitude of waveform spectrum under the MTIC with power limit. Leshem et al. assumed that all targets are taken from a Gaussian ensemble with known power spectral densities, and extended Bell's work to the case of multiple extended targets [13]. Also with the Gaussian assumption of target, clutter, and noise, the approach in [9] generalized the information theoretic water-filling method proposed by Bell to allow optimization for cluttering problems.

In the past decade, MIMO and cognitive radar developed rapidly by exploiting waveform diversity [14-22], and the waveform design methods under the MTIC were further investigated. In [14], the MI criterion and the mean square error criterion were employed for MIMO radar waveform design with Gaussian assumption, and it was shown that the two different criteria lead to the same result eventually. A comparison between the MI criterion and the relative entropy criterion [18, 19] was presented in [20], still assuming that the MIMO radar signal follows a Gaussian distribution. Combining the feedback loop in cognitive radar [16] and the MTIC, some representative results for adaptive waveform design were provided in [17] and [22].

It is difficult to obtain a closed-form expression of MI when the Gaussian assumption is not satisfied and it is even more difficult to estimate the joint probability density function of non-Gaussian distributed signals [23]. Therefore, all the

J. Zhang is the corresponding author.

H. Xu, J. Zhang, S. Wang, and C. Li are with the School of Electronic and Information Engineering, Beihang University, Beijing 100191, China (e-mail: xuhuaping@buaa.edu.cn, jwzhang@buaa.edu.cn).

W. Liu is with the Department of Electronic and Electrical Engineering, University of Sheffield, Sheffield S1 3JD, U.K. (e-mail: w.liu@sheffield.ac.uk).

waveform design problems studied under the MTIC in [9, 11-14, 17-20 and 22] assume that target, noise and clutter follow the Gaussian distribution.

Although the MTIC has been employed in various radar waveform design problems, to our best knowledge, it has not been investigated in terms of the high resolution requirement yet. Meanwhile, high resolution needs to be considered in many different types of radars [24-29]. For example, SAR with different platforms including spaceborne SAR, airborne SAR and unmanned aerial vehicle SAR, and many non-imaging radars, such as surveillance radar [24, 25], tracking radar [26, 27] and even weather radar [28, 29], all require a high resolution waveform. Therefore, the design of radar waveform meeting both high resolution and information acquisition requirements is of great importance in the aerospace field.

In this work, the high resolution waveform design problem under the MTIC is studied. By maximizing the Pearson correlation coefficient (PCC) for maximum information acquisition, a new expression for the objective function is derived without depending on the Gaussian assumption. With the constant power constraint to the waveform, a time-domain optimal solution is obtained for the resultant constrained optimization problem through reformulating the objective function as the well-known eigenvector problem. Then the resolution of the optimal waveform is analyzed. An information distortion criterion is defined to derive a suboptimal waveform meeting the high resolution requirement. The waveform is then evaluated in comparison with the classic LFMW given the same power and time-bandwidth product and it is shown that a better performance is achieved by the proposed design in terms of the peak sidelobe ratio (PSLR), information acquisition and classification.

The rest of paper is organized as follows. A system model is established in Section II for radar information acquisition and signal characterization, with the preliminary objective function under the MTIC introduced. In Section III, a Toeplitz matrix is used to represent the discrete signal model, and the optimization problem of maximizing the PCC under the constant power constraint is formulated. Then, the time-domain analytical solution is derived. Analyzing the bandwidth of the optimal waveform, the concept of information distortion is introduced and a suboptimal waveform is proposed with the tradeoff between resolution and information acquisition in Section IV. In Section V, the performance of the suboptimal waveform and LFMW is compared, and conclusions are drawn in Section VI.

## II. INFORMATION ACQUISITION MODEL OF RADAR

The radar information acquisition process can be modeled with a memoryless channel describing the information flow shown in Fig. 1. The target scattering characteristic function  $G(t)$  is a random process determining the information source, and interacts with the waveform function  $x(t)$  for spatial transmission. The modulated signal  $Z(t)$  is then corrupted by

additive noise  $N(t)$  to form the received signal  $Y(t)$  through an ideal bandpass filter  $b_f(t)$ . As a result, we have

$$Y(t) = [G(t) \otimes x(t) + N(t)] \otimes b_f(t), \quad (1)$$

where  $\otimes$  denotes the linear convolution operator. Lowercase letter and uppercase letter are used to represent deterministic signal and random process, respectively.

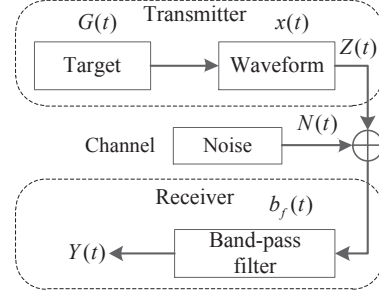


Figure 1. Information acquisition model for radar.

Based on the information theory, the mutual information  $I[Y(t); G(t)]$  between  $G(t)$  and  $Y(t)$  indicates how much information of target can be obtained by radar from the observed signal  $Y(t)$ . Therefore, the MTIC is to maximize  $I[Y(t); G(t)]$ , and the objective function is established as

$$\max \{I[Y(t); G(t)]\}. \quad (2)$$

Since  $x(t)$  is a deterministic signal,  $\max \{I[Y(t); G(t)]\}$  is equivalent to  $\max \{I[Y(t); Z(t)]\}$  [12].

However, finding a solution for  $\max \{I[Y(t); Z(t)]\}$  is a notoriously difficult task and infeasible in most realistic cases [30, 31]. Hence, it is necessary to transform the objective function in (2) into an equivalent new form.

In many practical problems of engineering optimization, maximizing PCC  $|\rho_{Y(t)Z(t)}|$  is a way to maximize mutual information [32], no matter what kind of distributions these random variables follow, i.e.

$$\max \{|\rho_{Y(t)Z(t)}|\} \Rightarrow \max \{I[Y(t); Z(t)]\}. \quad (3)$$

Therefore, the PCC is introduced to represent the objective function for waveform design under MTIC in this paper, and the corresponding constrained optimization problem is written as

$$\max_{x(t)} \{|\rho_{Y(t)Z(t)}|\} \quad \text{s.t. } x(t) \in \mathcal{D}, \quad (4)$$

where  $\mathcal{D}$  denotes the constraint set or feasible set of  $x(t)$ . Since the radar waveform must be limited in energy or power and provide high resolution in most practical applications, constant power and high resolution constraints are introduced to the objective function. Therefore, they are included in the set  $\mathcal{D}$ .

In the following analysis, without causing confusion and also due to the stationarity assumption of radar signal and noise, we will drop the time parameter  $t$  in the corresponding expressions.

### III. OPTIMAL WAVEFORM DERIVATION UNDER THE MTIC WITH POWER CONSTRAINT

Discrete-time processing of continuous-time signals is commonplace in bandlimited systems, such as radar, sonar and communication systems. To design a discrete radar waveform directly can circumvent the approximation issue [33, 34] caused by analog to digital conversion during signal processing at the receiver, compared with an analog waveform. Therefore, to facilitate signal processing and simulation on a digital computer, we directly present the waveform design in a discrete-time formulation of the signal model. The discrete version of the signals is considered, where  $\mathbf{g} \in \mathbb{C}^{l \times 1}$ ,  $\mathbf{x} \in \mathbb{C}^{n \times 1}$ ,  $\mathbf{b} \in \mathbb{C}^{n \times 1}$ ,  $\mathbf{n}' \in \mathbb{C}^{m \times 1}$ ,  $\mathbf{n} \in \mathbb{C}^{m \times 1}$  and  $\mathbf{y} \in \mathbb{C}^{m \times 1}$  denote the discretized target scattering, waveform, ideal bandpass filter, additive noise, bandpass filtered additive noise and the received signal, respectively. Since  $b_f(t)$  is supposed to be an ideal filter, so all signals within the passband of  $b_f(t)$  can pass through it without attenuation. Corresponding to (1), the discrete signal model can be expressed as

$$\begin{aligned} \mathbf{y} &= [\mathbf{g} \otimes \mathbf{x} + \mathbf{n}'] \otimes \mathbf{b} \\ &= \mathbf{g} \otimes \mathbf{x} \otimes \mathbf{b} + \mathbf{n}' \otimes \mathbf{b} \\ &= \mathbf{g} \otimes \mathbf{x} + \mathbf{n} = \mathbf{z} + \mathbf{n}, \end{aligned} \quad (5)$$

where  $\mathbf{g} = [g(0), g(1), \dots, g(l-1)]^T$ . The linear convolution operator can be implemented through a Toeplitz matrix defined as

$$\mathbf{G} = \begin{bmatrix} g(0) & 0 & \dots & \dots & 0 \\ g(1) & g(0) & \ddots & \dots & 0 \\ \vdots & \vdots & \ddots & \ddots & \vdots \\ g(l-1) & g(l-2) & \dots & g(0) & 0 \\ 0 & g(l-1) & g(l-2) & \dots & g(0) \\ \vdots & 0 & g(l-1) & \dots & g(1) \\ \vdots & \vdots & 0 & \ddots & \vdots \\ 0 & 0 & \dots & 0 & g(l-1) \end{bmatrix} \quad (6)$$

where  $\mathbf{G} \in \mathbb{C}^{m \times n}$  is the Toeplitz matrix of  $\mathbf{g}$  using  $n = l + 1$  as an example. Then, (5) is transformed into

$$\mathbf{y} = \mathbf{G}\mathbf{x} + \mathbf{n} = \mathbf{z} + \mathbf{n}. \quad (7)$$

Let  $\mathbf{m}_y$  and  $\mathbf{m}_z$  represent the mean value of  $\mathbf{y}$  and  $\mathbf{z}$ , respectively, and  $E[\cdot]$  represents the expectation operation. Assume that noise is of zero mean and independent of the signal associated with the target, so that  $\mathbf{m}_y = \mathbf{m}_z$ . Therefore, the PCC of  $\mathbf{y}$  and  $\mathbf{z}$  can be derived as

$$\begin{aligned} \rho_{YZ} &= \frac{E[(\mathbf{y} - \mathbf{m}_y)^H (\mathbf{z} - \mathbf{m}_z)]}{\sqrt{E[(\mathbf{y} - \mathbf{m}_y)^H (\mathbf{y} - \mathbf{m}_y)] E[(\mathbf{z} - \mathbf{m}_z)^H (\mathbf{z} - \mathbf{m}_z)]}} \\ &= \frac{\sqrt{\mathbf{x}^H E[\mathbf{G}^H \mathbf{G}] \mathbf{x} - |\mathbf{m}_y|^2}}{\sqrt{\sigma_N^2 + \mathbf{x}^H E[\mathbf{G}^H \mathbf{G}] \mathbf{x} - |\mathbf{m}_y|^2}}. \end{aligned} \quad (8)$$

(8) is further simplified into

$$|\rho_{YZ}|^2 = 1 - \frac{\sigma_N^2}{\sigma_N^2 + \mathbf{x}^H \mathbf{R}_G \mathbf{x}}, \quad (9)$$

where  $\sigma_N^2 = E[\mathbf{n}^H \mathbf{n}]$  and  $\mathbf{R}_G = E[\mathbf{G}^H \mathbf{G}] - [E(\mathbf{G})]^H E(\mathbf{G})$  defined as target feature matrix. If both constant power and high resolution constraints are imposed on the objective function at the same time, the constrained optimization problem will become quite complicated. So we first consider the constant power constraint and present a relaxed version of (4), leading to the following optimization problem

$$\max_{\mathbf{x}} \{\mathbf{x}^H \mathbf{R}_G \mathbf{x}\} \quad \text{s.t. } \mathbf{x}^H \mathbf{x} = 1. \quad (10)$$

In [35-37], a similar form of constrained optimization for waveform design is mentioned, i.e.

$$\max_{\mathbf{x}} \{\mathbf{x}^H \mathbf{R}_n^{-1} \mathbf{x}\} \quad \text{s.t. } \mathbf{x}^H \mathbf{x} = 1, \quad (11)$$

where  $\mathbf{R}_n^{-1}$  denotes the correlation matrix of colored noise, and it was derived under the criterion of maximizing signal-to-interference-plus-noise-ratio (SINR). It can be seen that (10) and (11) have different physical meanings, because (11) is focused on whitening colored noise instead of target feature enhancement in (10).

(10) can be viewed as an eigenvector problem, and the optimal waveform  $\mathbf{x}_{opt}$  under the constant power constraint is the eigenvector associated with the maximum eigenvalue of  $\mathbf{R}_G$ , i.e.

$$\mathbf{x}_{opt} = \underset{\max(\lambda)}{\text{eig}}(\mathbf{R}_G), \quad (12)$$

where  $\underset{\max(\lambda)}{\text{eig}}(\cdot)$  denotes the eigenvector corresponding to the largest eigenvalue  $\lambda$ .

### IV. HIGH RESOLUTION WAVEFORM DESIGN UNDER MTIC

High resolution is one key requirement for the radar waveform [38], especially for imaging radar systems. The results in Section III indicate that the optimal waveform based on the MTIC is the eigenvector corresponding to the largest eigenvalue of  $\mathbf{R}_G$ . Nevertheless, it is necessary to analyze the spectrum of eigenvectors when considering the resolution constraint since resolution depends on bandwidth of the waveform. It is found that the bandwidth of  $\mathbf{x}_{opt}$  does not usually meet the resolution requirement. Consequently, a new parameter called information distortion is defined, to show the tradeoff between information acquisition and resolution. In the following, a waveform design method is presented to accommodate the resolution requirement.

#### A. Bandwidth Analysis of the Optimal Waveform

The eigenvectors  $\mathbf{u}_0, \mathbf{u}_1, \dots, \mathbf{u}_{n-1}$  of  $\mathbf{R}_G$  can be regarded as the basis vectors of the space  $\mathbb{C}^n$ , and the corresponding eigenvalues are real-valued and sorted as  $\lambda_0 \geq \lambda_1 \geq \dots \geq \lambda_{n-1} \geq 0$ . Since  $\mathbf{R}_G$  is a semi-positive Hermitian matrix, it can be eigen-decomposed into

$$\begin{aligned} \mathbf{R}_G &= \sum_{i=0}^{n-1} \lambda_i \mathbf{u}_i \mathbf{u}_i^H \\ &= \sum_{i=0}^d \lambda_i \mathbf{u}_i \mathbf{u}_i^H + \sum_{i=d+1}^{n-1} \lambda_i \mathbf{u}_i \mathbf{u}_i^H, \end{aligned} \quad (13)$$

where  $d$  is an integer that satisfies  $0 \leq d < n - 1$ . For a small positive number  $\delta_1$ , we can find a  $d$ , so that  $\left\| \mathbf{R}_G - \sum_{i=0}^d \lambda_i \mathbf{u}_i \mathbf{u}_i^H \right\|_F^2 \leq \delta_1$ . The superscript  $\|\cdot\|_F^2$  denotes the Frobenius norm. With the representation

$$\sum_{i=d+1}^{n-1} \lambda_i \mathbf{u}_i \mathbf{u}_i^H = e(\delta_1), \quad (14)$$

we have

$$\mathbf{R}_G = \sum_{i=0}^d \lambda_i \mathbf{u}_i \mathbf{u}_i^H + e(\delta_1), \quad (15)$$

where  $e(\delta_1)$  denotes the error term related to  $\delta_1$ . Applying discrete Fourier transform (DFT) column-wise to (15) leads to

$$\begin{aligned} \mathbf{W}^H \mathbf{R}_G &= \mathbf{W}^H \sum_{i=0}^d \lambda_i \mathbf{u}_i \mathbf{u}_i^H + \mathbf{W}^H e(\delta_1) \\ &= \sum_{i=0}^d \lambda_i \begin{bmatrix} \mathbf{w}_0^H \\ \mathbf{w}_1^H \\ \vdots \\ \mathbf{w}_{n-1}^H \end{bmatrix} \mathbf{u}_i \mathbf{u}_i^H + \mathbf{W}^H e(\delta_1) \\ &= \sum_{i=0}^d \lambda_i \begin{bmatrix} \langle \mathbf{u}_i, \mathbf{w}_0 \rangle \\ \langle \mathbf{u}_i, \mathbf{w}_1 \rangle \\ \vdots \\ \langle \mathbf{u}_i, \mathbf{w}_{n-1} \rangle \end{bmatrix} \mathbf{u}_i^H + \mathbf{W}^H e(\delta_1) \end{aligned} \quad (16)$$

where  $\langle \cdot \rangle$  is the vector inner product and  $\mathbf{W}$  is the DFT matrix, and

$$\begin{aligned} \mathbf{W} &= [\mathbf{w}_0, \mathbf{w}_1, \dots, \mathbf{w}_{n-1}] \\ &= \begin{bmatrix} 1 & 1 & \dots & 1 \\ 1 & w^1 & \dots & w^{(n-1)} \\ \vdots & \vdots & \ddots & \vdots \\ 1 & w^{(n-1)} & \dots & w^{(n-1)^2} \end{bmatrix}. \end{aligned} \quad (17)$$

$[\mathbf{w}_0, \mathbf{w}_1, \dots, \mathbf{w}_{n-1}]$  is the Fourier bases of space  $\mathbb{C}^n$ , where  $w = e^{j2\pi/n}$  and  $\mathbf{w}_k$ ,  $0 \leq k \leq n - 1$ , is the  $k$ -th column vector of  $\mathbf{W}$ . The contribution of  $\mathbf{W}^H e(\delta_1)$  in (16) to signal spectrum is negligible. Then, we have

$$\mathbf{W}^H \mathbf{R}_G \approx \sum_{i=0}^d \lambda_i \begin{bmatrix} \langle \mathbf{u}_i, \mathbf{w}_0 \rangle \\ \langle \mathbf{u}_i, \mathbf{w}_1 \rangle \\ \vdots \\ \langle \mathbf{u}_i, \mathbf{w}_{n-1} \rangle \end{bmatrix} \mathbf{u}_i^H. \quad (18)$$

$\mathbf{R}_G$  can be viewed as a two-dimensional baseband signal related to the spectrum of target scattering. The eigenvectors  $\mathbf{u}_i$  ( $i = 0, 1, \dots, d$ ) corresponding to large eigenvalues have intense response to the low frequency Fourier bases and very small projection coefficients on the high frequency bases. There must exist a  $v$  with  $0 \leq v < n - 1$  and for all  $i = 0, 1, \dots, d$  and  $j = v, v + 1, \dots, n - 1$ ,  $\max |\langle \mathbf{u}_i, \mathbf{w}_j \rangle| \leq \delta_2$  with a small positive number  $\delta_2$ .

All eigenvectors of the target feature matrix  $\mathbf{R}_G$  form the standard orthogonal bases of space  $\mathbb{C}^n$  and the spectrum of them will cover all frequency components of the unitary space.

The spectrum of eigenvectors corresponding to large eigenvalues always cover the low frequency range, because  $\mathbf{R}_G$  is a baseband signal. Since multiple eigenvectors are orthogonal to each other, their spectra do not overlap completely. So the single eigenvector  $\mathbf{u}_0$  can only cover part of the total spectrum of  $\mathbf{R}_G$ . We use the Monte Carlo method to simulate an extended target with a certain statistical distribution and bandwidth  $\pi$  rad, and then calculate  $\mathbf{R}_G$  and  $\mathbf{u}_0$ . The spectrum of  $\mathbf{u}_0$  is shown in Fig. 2. It can be observed that the 3dB bandwidth of  $\mathbf{u}_0$  is very narrow and only cover 0.0212rad.

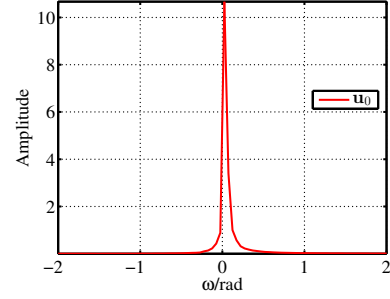


Figure 2. The spectrum of eigenvector  $\mathbf{u}_0$ . The amplitude of target scattering follows the Rayleigh distribution with the parameter 0.5.

From the above spectrum analysis of eigenvectors, it is concluded that the optimal waveform  $\mathbf{u}_0$  under the MTIC may not meet the resolution requirement. Therefore, a suboptimal waveform design method is proposed below to find a tradeoff between resolution improvement and information acquisition.

### B. High Resolution Waveform Design Under the MTIC

In order to overcome the limited bandwidth of the optimal waveform  $\mathbf{u}_0$ , a combination of multiple eigenvectors associated with large eigenvalues is employed. Although the bandwidth is increased by introducing more eigenvectors, information acquisition will be reduced, due to the influence of the eigenvectors of small eigenvalues. In consequence, this combination is expected to guarantee that resolution satisfies the requirement while the information acquisition ability does not degrade too much.

In the following, information distortion is defined to give a tradeoff between information acquisition and resolution as follows

$$\begin{aligned} \Delta &= \frac{\mathbf{u}_0^H \mathbf{R}_G \mathbf{u}_0 - \mathbf{x}_{sopt}^H \mathbf{R}_G \mathbf{x}_{sopt}}{\mathbf{u}_0^H \mathbf{R}_G \mathbf{u}_0} \\ &= 1 - \frac{\mathbf{x}_{sopt}^H \mathbf{R}_G \mathbf{x}_{sopt}}{\lambda_0} \end{aligned} \quad (19)$$

where  $\mathbf{x}_{sopt} \in \mathbb{C}^{n \times 1}$  denotes the suboptimal waveform that satisfies power and resolution constraints simultaneously. It is clear that the distortion of  $\mathbf{u}_0$  is 0. Since any  $n$ -dimensional vector can be projected onto the whole set of eigenvectors, it follows that

$$\mathbf{x}_{sopt} = \sum_{i=0}^{n-1} q_i \mathbf{u}_i \quad (20)$$

where  $q_i \in \mathbb{C}$  represents the projection coefficient for  $\mathbf{u}_i$ . Substituting (20) into (19), we have

$$\Delta_{s_{opt}} = 1 - \frac{\sum_{i=0}^{n-1} \lambda_i |q_i|^2}{\lambda_0}. \quad (21)$$

Therefore, the most dominant factor affecting the distortion is the projection coefficient or weight. Different weight will generate different distortion leading to a different suboptimal waveform. Following this idea, a suboptimal waveform design method is given below.

The eigenvalues are used to weight the corresponding eigenvectors directly, i.e.  $q_i = \lambda_i / \sqrt{\sum_{i=0}^{n-1} \lambda_i^2}$ , leading to a suboptimal waveform, given by

$$\mathbf{x}_{s_{opt}} = \sum_{i=0}^{n-1} q_i \mathbf{u}_i = \frac{1}{\sqrt{\sum_{i=0}^{n-1} \lambda_i^2}} \sum_{j=0}^{n-1} \lambda_j \mathbf{u}_j. \quad (22)$$

According to the objective function and the distortion, the larger the eigenvalue of  $\mathbf{R}_G$ , the larger the amount of information obtained by the corresponding eigenvector and accordingly the smaller the distortion. The magnitude of each eigenvalue reflects the information acquisition capability of the corresponding eigenvector serving as the chosen waveform. Using the eigenvalues as weighting factors is consistent with this observation.

The distortion of  $\mathbf{x}_{s_{opt}}$  is

$$\Delta_{\mathbf{x}_{s_{opt}}} = 1 - \frac{1}{\lambda_0} \sum_{i=0}^{n-1} \lambda_i |q_i|^2 = 1 - \frac{1}{\lambda_0 \sum_{i=0}^{n-1} \lambda_i^2} \sum_{j=0}^{n-1} \lambda_j^3. \quad (23)$$

$\Delta_{\mathbf{x}_{s_{opt}}}$  in (23) is possible to exceed the maximum distortion allowed by system. Distortion reduction can be achieved by removing several insignificant eigenvectors associated with small eigenvalues. Let  $\tilde{\mathbf{x}}_{s_{opt}}$  denote the modified waveform; it can be expressed as

$$\begin{aligned} \tilde{\mathbf{x}}_{s_{opt}} &= \frac{1}{\sqrt{\sum_{i=0}^{K-1} \lambda_i^2}} \sum_{j=0}^{K-1} \lambda_j \mathbf{u}_j \\ &= \frac{1}{\sqrt{\sum_{i=0}^{K-1} |q_i|^2}} \sum_{j=0}^{K-1} q_j \mathbf{u}_j, \quad 1 \leq K < n-1. \end{aligned} \quad (24)$$

Its information distortion is

$$\Delta_{\tilde{\mathbf{x}}_{s_{opt}}} = 1 - \frac{1}{\lambda_0 \sum_{i=0}^{K-1} |q_i|^2} \sum_{j=0}^{K-1} \lambda_j |q_j|^2 = 1 - \frac{1}{\lambda_0 \sum_{i=0}^{K-1} \lambda_i^2} \sum_{j=0}^{K-1} \lambda_j^3. \quad (25)$$

Comparing (23) and (25), the difference is given by

$$\Delta_{\mathbf{x}_{s_{opt}}} - \Delta_{\tilde{\mathbf{x}}_{s_{opt}}} = \frac{1}{\lambda_0 \sum_{i=0}^{K-1} |q_i|^2} \sum_{j=0}^{K-1} \lambda_j |q_j|^2 - \frac{1}{\lambda_0} \sum_{i=0}^{n-1} \lambda_i |q_i|^2. \quad (26)$$

Because  $\lambda_0 \geq \lambda_1 \geq \dots \geq \lambda_{n-1} \geq 0$ , we have

$$\begin{aligned} &\lambda_0 (\Delta_{\mathbf{x}_{s_{opt}}} - \Delta_{\tilde{\mathbf{x}}_{s_{opt}}}) \\ &\geq \frac{1}{\sum_{i=0}^{K-1} |q_i|^2} \sum_{j=0}^{K-1} \lambda_j |q_j|^2 - \left( \sum_{i=0}^{K-1} \lambda_i |q_i|^2 + \lambda_K \sum_{i=K}^{n-1} |q_i|^2 \right) \\ &= \sum_{j=0}^{K-1} \lambda_j \left( \frac{|q_j|^2}{\sum_{i=0}^{K-1} |q_i|^2} - |q_j|^2 \right) - \lambda_K \left( 1 - \sum_{j=0}^{K-1} |q_j|^2 \right). \end{aligned} \quad (27)$$

With  $\sum_{i=0}^{K-1} |q_i|^2 \leq 1$ , (27) changes to

$$\begin{aligned} &\sum_{j=0}^{K-1} \lambda_j \left( \frac{|q_j|^2}{\sum_{i=0}^{K-1} |q_i|^2} - |q_j|^2 \right) - \lambda_K \left( 1 - \sum_{j=0}^{K-1} |q_j|^2 \right) \\ &\geq \lambda_K \left( \frac{\sum_{j=0}^{K-1} |q_j|^2}{\sum_{i=0}^{K-1} |q_i|^2} - \sum_{j=0}^{K-1} |q_j|^2 \right) - \lambda_K \left( 1 - \sum_{j=0}^{K-1} |q_j|^2 \right) = 0. \end{aligned} \quad (28)$$

Finally, we have

$$\Delta_{\mathbf{x}_{s_{opt}}} - \Delta_{\tilde{\mathbf{x}}_{s_{opt}}} \geq 0. \quad (29)$$

The above equations show that the distortion is reduced as  $K$  decreases. Therefore, the adjustment of  $K$  is a way to find the suitable tradeoff between distortion and resolution in the design of  $\mathbf{x}_{s_{opt}}$ . However, a quantitative relationship between bandwidth, distortion and  $K$  cannot be found in a closed-form. So a numerical method is proposed.

Step 1: Using the a priori knowledge of targets to obtain  $\mathbf{R}_G$ , and then its eigenvalues and eigenvectors are obtained by eigen-decomposition.

Step 2: The eigenvalues are used to weight the corresponding eigenvectors, generating  $\mathbf{x}_{s_{opt}K}$  which represents a set of suboptimal waveforms with respect to each value of  $K$ , and then draw a figure to show the bandwidth and distortion with respect to the value of  $K$  from 0 to  $n-1$ .

Step 3: Based on the requirements for certain bandwidth and distortion, find a suitable  $K$  from the figure given in Step 2.

Without loss of generality, if the largest eigenvalue is much larger than the others, then the eigenvectors corresponding to very small eigenvalues would make little contribution to the final suboptimal waveform and fail to broaden the bandwidth of the waveform. Therefore, we could consider the logarithm of corresponding eigenvalues as the weight.

## V. SIMULATION RESULTS AND ANALYSIS

In this section, Monte Carlo simulations are performed to verify the theoretical analysis and assess the performance of the suboptimal waveform. Firstly, the theoretical analyses in Section III and Section IV are validated by comparing the information acquisition capability of different eigenvectors,

Table I  
EXPERIMENTAL PARAMETERS

Parameter	Symbols	Numerical Value
Rayleigh: $f( g ) = \frac{ g }{\sigma^2} \exp\left(-\frac{ g ^2}{2\sigma^2}\right)$	$\sigma$	0.5
Weibull: $f( g ) = \frac{c g ^{c-1}}{b^c} \exp\left(-\left(\frac{ g }{b}\right)^c\right)$	$b$	1
	$c$	1.5
Phase: $f(\theta) = \frac{1}{\theta_2 - \theta_1}, \theta \in [\theta_1, \theta_2]$	$\theta_1$	$-\pi$
	$\theta_2$	$\pi$
The mean of $G(t)$	$m_G$	0
Sample frequency	$f_S$	100MHz
LFMW duration	$\tau$	1.28 $\mu$ s
Waveform bandwidth	$B$	30MHz

and presenting the distortion and bandwidth with respect to the value of  $K$ . Then, the proposed waveform is evaluated in comparison with the classic LFMW given the same power and time-bandwidth product. The PCC, misclassification probability, ambiguity function and correlation function are used as performance indexes for information acquisition, classification and resolution, respectively. In practice, most targets cannot be considered as point targets and point targets are also a special case of extended targets. Therefore, we evaluate the performance based on extended targets whose scattering amplitude follows Rayleigh [39] and Weibull distributions [40, 41], respectively, and phase<sup>1</sup> is uniformly distributed. The main parameters are listed in Table I.

Details of the simulation process are given below:

1) Setting  $n = 128$ ,  $l = 10^6$  target scattering samples as one group for estimating  $\mathbf{R}_G$  and designing the waveform are generated randomly obeying Rayleigh and Weibull distributions as listed in Table I, respectively.  $\mathbf{R}_G$  is calculated by  $\mathbf{R}_G = E[\mathbf{G}^H \mathbf{G}] - [E(\mathbf{G})]^H E(\mathbf{G})$  and its eigenvalues and eigenvectors are obtained, which are then used to find  $\mathbf{x}_{sopt}$  with  $K$  determined by Steps 1-3 in Section IV. B.

2) Using the same parameters as in 1),  $N = 500$  groups of target scattering samples are generated to serve as testing sets to verify the theoretical analysis and evaluate the performance, where  $\mathbf{u}_0$ ,  $\mathbf{u}_5$ ,  $\mathbf{u}_{10}$ ,  $\mathbf{x}_{sopt}$  and LFMW  $\mathbf{c}_P$  act as transmitting waveforms respectively. The echo is formed after the target is observed and noise according to different SNR requirements is added.

3) Afterwards, performances of the proposed suboptimal waveform and the LFMW are compared and analyzed using the echo of different waveforms and filtering results.

#### A. Theoretical Analysis Verification

First of all, the result in (12) is validated, while showing the amount of information  $|\rho_{YZ}|^2$  acquired by waveforms  $\mathbf{u}_0$ ,  $\mathbf{u}_5$  and  $\mathbf{u}_{10}$  with different SNRs and statistical distributions.  $\mathbf{u}_0$  is the optimal waveform under MTIC and chosen as the benchmark, then  $\mathbf{u}_5$  and  $\mathbf{u}_{10}$  are chosen arbitrarily.  $|\rho_{YZ}|^2$  of the three waveforms under the SNR from -10 to 10dB is given below. Fig. 3(a) shows the value of  $|\rho_{YZ}|^2$  for Rayleigh distribution, and the corresponding simulation result of Weibull distribution is shown in Fig. 3(b).

<sup>1</sup>Using a random variable  $\theta$  to represent the phase of  $G(t)$  and it is uniformly distributed on  $[\theta_1, \theta_2]$  [1,12].

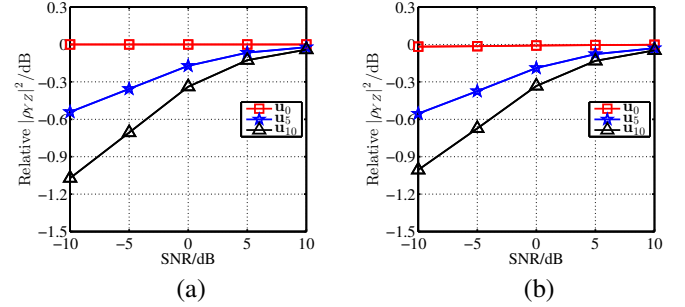


Figure 3. Information acquisition comparison of the three eigenvectors with different distributions: (a) Rayleigh distribution; (b) Weibull distribution. The relative value of  $|\rho_{YZ}|^2$  is converted into decibel by considering  $\mathbf{u}_0$  corresponding to the Rayleigh distribution as the benchmark.

It can be seen that information acquisition by  $\mathbf{u}_0$  is better than the other two eigenvectors. Moreover, it is found that the results for Rayleigh and Weibull distributions are almost identical. As mentioned above,  $|\rho_{YZ}|^2$  is mainly determined by  $\mathbf{x}^H \mathbf{R}_G \mathbf{x}$ , and  $\mathbf{R}_G$  depends on the second-order statistics of  $G(t)$ . So if the second-order statistics of scattering characteristic are the same, then the value of  $|\rho_{YZ}|^2$  will not show much difference.

In order to verify the design of suboptimal waveform given in (19)-(29), the relationship between bandwidth, distortion and the number of eigenvectors  $K$  defined in (24) is presented in Fig. 4.

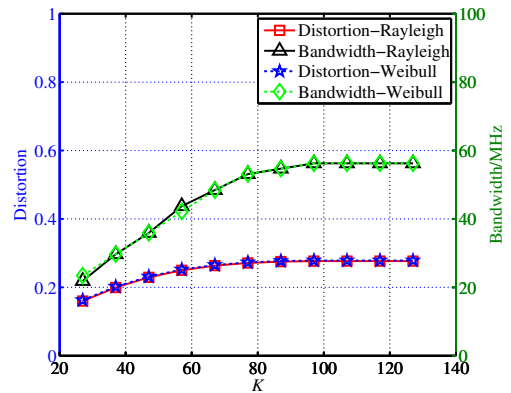


Figure 4. The relationship between bandwidth, distortion and the number of eigenvectors  $K$ .

It can be found that the distortion and bandwidth are both increased with the increase of  $K$ , which is consistent with

our analysis. Using Steps 1-3 in Section IV. B, the value of  $K$  is determined as  $K = 39$  for both Rayleigh and Weibull distributions. Then  $\mathbf{x}_{sopt}$  is generated with the corresponding  $K$ , and its energy spectrum density (ESD) is shown in Fig. 5.

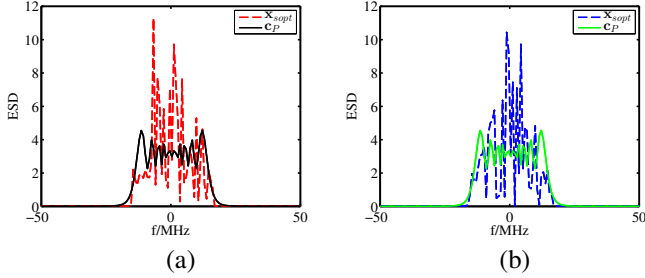


Figure 5. The ESD of  $\mathbf{x}_{sopt}$  and the LFMW  $\mathbf{c}_P$  with  $\mathbf{x}_{sopt}^H \mathbf{x}_{sopt} = \mathbf{c}_P^H \mathbf{c}_P = 1$ : (a) Rayleigh distribution; (b) Weibull distribution.

### B. Performance Assessment

Next, under the condition of constant power and same time-bandwidth product, information acquisition, classification and resolution are evaluated for the suboptimal waveform and LFMW.

1) *Information Acquisition*: First, the information acquisition performance of  $\mathbf{x}_{sopt}$  and  $\mathbf{c}_P$  is compared with similar parameters to Fig. 3. The values of  $|\rho_{YZ}|^2$  for these waveforms are shown in Fig. 6.

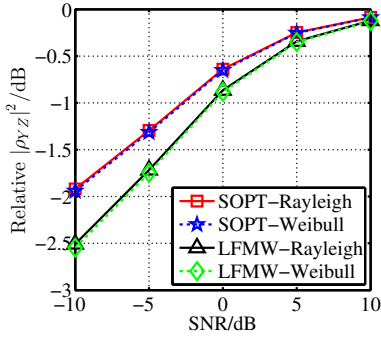


Figure 6. Information acquisition evaluation result for Rayleigh and Weibull distributions. The relative value of  $|\rho_{YZ}|^2$  is converted into decibel by considering  $\mathbf{u}_0$  corresponding to the Rayleigh distribution as the benchmark.

It can be seen that  $\mathbf{x}_{sopt}$  with both Rayleigh and Weibull distributions has achieved better result than LFMW  $\mathbf{c}_P$ . Referring to Fig. 3, although the value of  $|\rho_{YZ}|^2$  for  $\mathbf{x}_{sopt}$  is not as good as that of  $\mathbf{u}_0$ , this suboptimal waveform still acquire higher amount of information than  $\mathbf{c}_P$ . By contrast, the maximum gap of  $|\rho_{YZ}|^2$  between  $\mathbf{c}_P$  and  $\mathbf{x}_{sopt}$  with the Rayleigh distribution is about 0.5893dB, and 0.6057dB for Weibull distribution.

2) *Classification*: Fano's inequality provides a mathematical means to relate the mutual information between  $N_C$  types of targets  $\mathbf{t}$  and system output  $\mathbf{p}$  to a lower bound on the probability of misclassification  $P_E$  and can be written as an equality [2]

$$H(\mathbf{t}) - I(\mathbf{t}; \mathbf{p}) = \varepsilon + H(P_E) + P_E \log(N_C - 1) \quad (30)$$

where  $H(\cdot)$  denotes entropy, and  $\varepsilon$  is a bias offset. Therefore, the probability of misclassification  $P_E$  can also measure the information acquisition performance.

In order to further assess the performance of  $\mathbf{x}_{sopt}$ , we consider the problem of target classification. Referring to Fig. 1, a radar classification system can be simplified into Fig. 7. Here the signal  $\mathbf{r}$  is processed by matched filtering to suppress noise and achieve a high resolution.

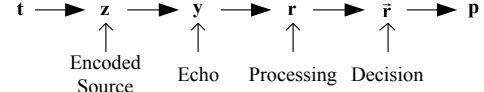


Figure 7. Radar classification system.

Two types of extended targets with the same statistical distribution are illuminated by the transmitted waveforms respectively, and the probability of misclassification is calculated. The two types of extended targets have different variances (1 and 2), but their other parameters are the same. It is assumed that there are two radar systems with exactly the same parameters except for the employed waveform, which is  $\mathbf{x}_{sopt}$  and  $\mathbf{c}_P$ , respectively. Classification is performed based on  $\mathbf{r}$  after pulse compression.

Before classification is performed, it is necessary to determine the decision threshold.  $\mathbf{x}_{sopt}$  is taken as an example to show the process.  $N$  sets of samples of the first and the second types of targets form two different scenes, respectively (called Scene 1 and Scene 2). The suboptimal waveform  $\mathbf{x}_{sopt}$  is designed only for the first type of targets. Observing Scene 1 and Scene 2 separately without noise,  $N$  groups of power signals  $|\mathbf{r}|^2$  for each scene, can be obtained after filtering. The average of the mean values of the two scenes power signal  $|\mathbf{r}|^2$  is considered as the threshold.

$N$  random numbers containing only 0 and 1 are generated to form a target sequence  $\mathbf{t}$  randomly, where 0 represents the first type of targets and 1 represents the second. According to the sequence  $\mathbf{t}$ ,  $N$  sets of scattering samples containing two types of targets are generated and recorded as Scene 0. The two radars observe Scene 0 at the same time, and the classification results  $\mathbf{p}$  are obtained respectively. Then, each element of  $\mathbf{p}$  and  $\mathbf{t}$  is compared, and the misclassification probabilities for the two waveforms are computed and shown in Fig. 8.

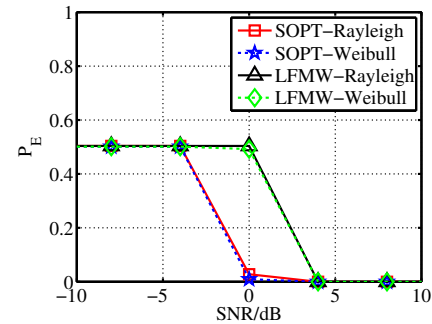


Figure 8. The misclassification probability of the two waveforms. The decision thresholds of  $\mathbf{x}_{sopt}$  and  $\mathbf{c}_P$  following the Rayleigh distribution are 44.543 and 22.255, respectively, and they are 41.0357 and 22.0075 corresponding to Weibull distribution.

It can be seen that the misclassification probability for  $\mathbf{x}_{sopt}$  is smaller than that for  $\mathbf{c}_P$  under the two different distributions. So  $\mathbf{x}_{sopt}$  has a superior noise suppressing performance for extended targets. When the SNR decreases to 0dB, the above two types of targets following the Rayleigh or Weibull distribution can still be distinguished correctly by  $\mathbf{x}_{sopt}$ , but the LFMW  $\mathbf{c}_P$  does not work well for discrimination. Moreover, it can be found that the misclassification probability of  $\mathbf{c}_P$  reaches a turning point when the SNR is increased to 4dB, which is roughly 4dB higher than  $\mathbf{x}_{sopt}$ . In summary, the probability of misclassification further indicates that  $\mathbf{x}_{sopt}$  has better information acquisition capability than  $\mathbf{c}_P$ .

3) *Resolution Evaluation*: The same bandwidth is set for all waveforms to compare their resolution performance. The three dimensional (3D) and two dimensional (2D) ambiguity function (AF), and correlation function (CF) are shown, respectively, in Figs. 9 and 10. The ambiguity function of  $\mathbf{x}_{sopt}$  for both statistical distributions is approximated as a pin shape with a single peak at zero delay and zero Doppler as shown in Fig. 9(a)-(d). Hence,  $\mathbf{x}_{sopt}$  has nearly ideal range-Doppler ambiguity properties. By contrast, the ambiguity function of  $\mathbf{c}_P$  in Fig. 9(e) and (f) looks like a blade, and there is coupling between range and Doppler due to the oblique triangle shape.

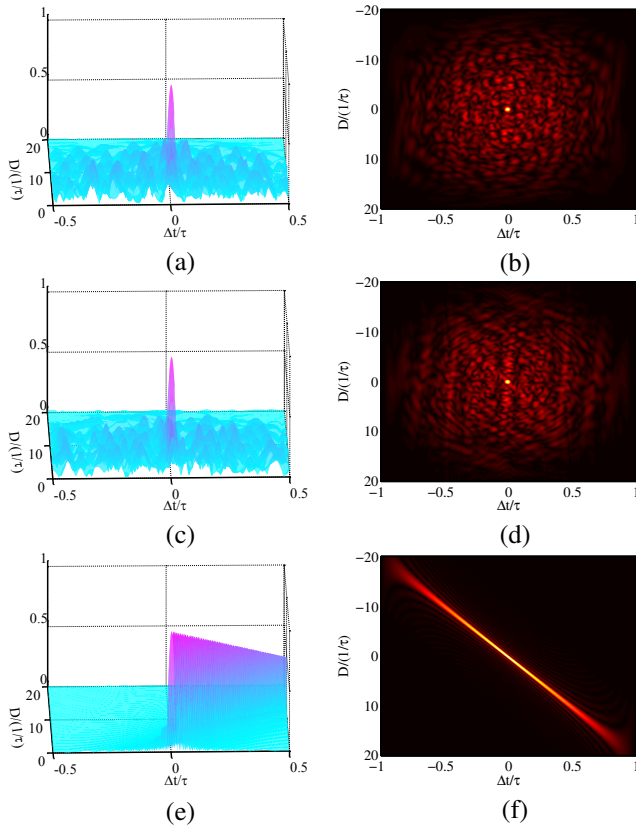


Figure 9. Partial 3D and 2D ambiguity function of  $\mathbf{x}_{sopt}$  with different distributions and LFMW  $\mathbf{c}_P$ : (a) 3D AF of  $\mathbf{x}_{sopt}$  (Rayleigh); (b) 2D AF of  $\mathbf{x}_{sopt}$  (Rayleigh); (c) 3D AF of  $\mathbf{x}_{sopt}$  (Weibull); (d) 2D AF of  $\mathbf{x}_{sopt}$  (Weibull); (e) 3D AF of LFMW; (f) 2D AF of LFMW.  $\Delta t$ ,  $D$  and  $\tau$  represent time delay, Doppler frequency shift, and duration, respectively.

To further compare spatial resolution of the three waveforms, the zero Doppler slice of the ambiguity function is

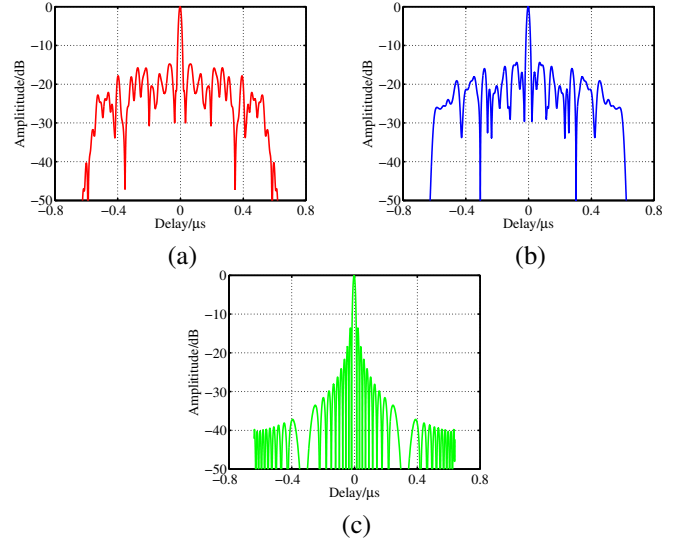


Figure 10. Correlation function of  $\mathbf{x}_{sopt}$  with different distributions and LFMW  $\mathbf{c}_P$ : (a) CF with the Rayleigh distribution; (b) CF with the Weibull distribution; (c) CF of LFMW  $\mathbf{c}_P$ .

chosen as shown in Fig. 10. Besides, their 3dB mainlobe width and PSLR are listed in Table II.

Table II  
RESOLUTION INDEXES

waveform	Index	3dB Mainlobe Width ( $\mu\text{s}$ )	PSLR(dB)
Rayleigh	$\mathbf{x}_{sopt}$	0.0174	-14.77
	$\mathbf{c}_P$	0.0141	-13.26
Weibull	$\mathbf{x}_{sopt}$	0.0174	-14.38
	$\mathbf{c}_P$	0.0141	-13.26

It is observed that the two suboptimal waveforms  $\mathbf{x}_{sopt}$  corresponding to Rayleigh and Weibull distributions have a slight loss of  $0.0033\mu\text{s}$  in resolution, compared with the same time-width product  $\mathbf{c}_P$ . But the suboptimal waveform has obtained a better PSLR. The PSLRs of  $\mathbf{x}_{sopt}$  (-14.77dB and -14.38dB) are both better than -13.26dB of  $\mathbf{c}_P$ . Although the suboptimal waveform experiences a decrease in mainlobe width to some extent,  $\mathbf{x}_{sopt}$  has a better ambiguity function and PSLR.

In summary, the waveforms designed by the proposed method under the MTIC can acquire higher amount of information and ultimately achieve a better classification result than the classic LFMW with the same power and time-bandwidth product. Results based on the resolution evaluation indexes indicate that the suboptimal waveform also has a high resolution.

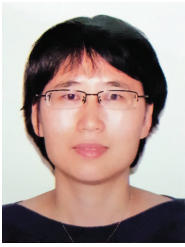
## VI. CONCLUSION

In this paper, a method of high resolution radar waveform design based on the MTIC for extended targets has been presented. A suboptimal transmit sequence with high information acquisition and resolution ability is obtained, and it is not limited by the Gaussian assumption on target statistics. An explicit objective function was first established by introducing PCC and the discrete-time analytical waveform under the constant

power constraint was derived; then the resolution requirement was considered in the constrained optimization problem and a suboptimal waveform design method was proposed based on the concept of information distortion; finally, performance of the suboptimal waveform and the LFMW was evaluated in terms of information acquisition, classification and resolution under the same time-bandwidth product and power. Numerical results have shown that the suboptimal waveform has better information acquisition, classification and a lower PSLR with a slightly degraded resolution than LFMW.

## REFERENCES

- [1] Frost, V. S., and Shanmugan, K. S., "The Information content of synthetic aperture radar images of terrain," *IEEE Transactions on Aerospace and Electronic Systems*, vol. AES-19, no. 5, pp. 768-774, 1983.
- [2] Malas, J. A., Cortese, J. A., and Ryan, P., "Uncertainty propagation and the Fano based information theoretic method," *2015 IEEE Radar Conference(RadarCon)*, pp. 1638-1643, 2015.
- [3] Moreira, A., Prats-Iraola, P., Younis, M., Krieger, G., and Hajnsek, I., "A tutorial on synthetic aperture radar," *IEEE Geoscience and Remote Sensing*, vol. 1, no. 1, pp. 6-43, 2013.
- [4] Tison, C., Nicolas, J. M., Tupin, F., and Maitre, H., "A new statistical model for Markovian classification of urban areas in high-resolution SAR images," *IEEE Transactions on Geoscience and Remote Sensing*, vol. 42, no. 10, pp. 2046-2057, 2004.
- [5] Levanon, N., and Mozeson, E., "Radar Signal," New York, NY, USA: Wiley, pp. 57-67, 2004.
- [6] Krieger, G., Gebert, N., and Moreira, A., "Multidimensional waveform encoding: A new digital beamforming technique for synthetic aperture radar remote sensing," *IEEE Transactions on Geoscience and Remote Sensing*, vol. 46, no. 1, pp. 31-46, 2008.
- [7] Krieger, G., "Opportunities and pitfalls," *IEEE Transactions on Geoscience and Remote Sensing*, vol. 52, no. 5, pp. 2628-2645, 2014.
- [8] Wang, W., "MIMO SAR OFDM chirp waveform diversity design with random matrix modulation," *IEEE Transactions on Geoscience and Remote Sensing*, vol. 53, no. 3, pp. 1615-1625, 2015.
- [9] Romero, R. A., Bae, J., and Goodman, N. A., "Theory and application of SNR and mutual information matched illumination waveforms," *IEEE Transactions on Aerospace and Electronic Systems*, vol. 47, no. 2, pp. 912-927, 2011.
- [10] Woodward, P. M., "Probability and information theory with applications to radar (Second Edition)," London, England: Pergamon pp. 62-80, 1964.
- [11] Bell, M. R., "Information theory and radar waveform design," *IEEE Transactions on Information Theory*, vol. 39, no. 5, pp. 1578-1597, 1993.
- [12] Bell, M. R., "Information theory and radar: Mutual information and the design and analysis of radar waveforms and systems," *Ph.D. dissertation*, Mar, California Institute of Technology, Pasadena, CA, 1988.
- [13] Leshem, A., Naparstek, O., and Nehorai, A., "Information theoretic adaptive radar waveform design for multiple extended targets," *IEEE Journal of Selected Topics in Signal Processing*, vol. 1, no. 1, pp. 42-55, 2007.
- [14] Yang, Y., and Blum, R. S., "Minimax robust MIMO radar waveform design," *IEEE Journal of Selected Topics in Signal Processing*, vol. 1, no. 1, pp. 147-155, 2007.
- [15] Maio, A. D., and Lops, M., "Design principles of MIMO radar detectors," *IEEE Transactions on Aerospace and Electronic Systems*, vol. 43, no. 3, pp. 886-898, 2007.
- [16] Haykin, S., "Cognitive radar: a way of the future," *IEEE Signal Processing*, vol. 23, no. 1, pp. 30-40, 2006.
- [17] Goodman, N. A., Venkata, P. R., and Neifeld, M. A., "Adaptive waveform design and sequential hypothesis testing for target recognition with active sensors," *IEEE Transactions on Signal Processing*, vol. 1, no. 1, pp. 105-113, 2007.
- [18] Kay, S., "Waveform design for multistatic radar detection," *IEEE Transactions on Aerospace and Electronic Systems*, vol. 45, no. 3, pp. 1153-1166, 2009.
- [19] Zhu, Z., Kay, S., and Raghavan, R. S., "Information-theoretic optimal radar waveform design," *IEEE Signal Processing Letters*, vol. 24, no. 3, pp. 274-278, 2017.
- [20] Tang, B., Tang, J., and Peng, Y., "MIMO radar waveform design in colored noise based on information theory," *IEEE Transactions on Signal Processing*, vol. 58, no. 9, pp. 4684-4697, 2010.
- [21] Huleihel, W., Tabrikian, J., and Shavit, R., "Optimal adaptive waveform design for cognitive MIMO radar," *IEEE Transactions on Signal Processing*, vol. 61, no. 20, pp. 5075-5089, 2013.
- [22] Liu, Y., Liao, G., Xu, J., Yang, Z. and Zhang, Y., "Adaptive OFDM integrated radar and communications waveform design based on information theory," *IEEE Communications Letters*, vol. 21, no. 10, pp. 2174-2177, 2017.
- [23] Zeng, X., and Durrani, T. S., "Estimation of mutual information using Copula density function," *Electronics Letters*, vol. 47, no. 8, pp. 493-494, 2011.
- [24] Petrov, N., Chevalier, F. L. and Yarovoy, A. G., "Detection of range migrating targets in compound-Gaussian clutter," *IEEE Transactions on Aerospace and Electronic Systems*, vol. 54, no. 1, pp. 37-50, 2018.
- [25] Stove, A. G. and Gashinova, M. S., "Passive maritime surveillance using satellite communication signals," *IEEE Transactions on Aerospace and Electronic Systems*, vol. 53, no. 6, pp. 2987-2997, 2017.
- [26] Jiang, N., Wu, R. and Li, J., "Super resolution feature extraction of moving targets," *IEEE Transactions on Aerospace and Electronic Systems*, vol. 37, no. 3, pp. 781-793, 2001.
- [27] Guo, Y., Li, Y., Tharmarsa, R., Kirubarajan, T., Efe, M. and Sarikaya, B., "GP-PDA filter for extended target tracking with measurement origin uncertainty," *IEEE Transactions on Aerospace and Electronic Systems*, vol. 55, no. 4, pp. 1725-1742, 2019.
- [28] McLaughlin, D. J., Knapp, E. A., Wang, Y. and Chandrasekar, V., "Distributed weather radar using X-band active arrays," *IEEE Transactions on Aerospace and Electronic Systems*, vol. 24, no. 7, pp. 21-26, 2009.
- [29] Hildebrand, P. H., Walther, G. and Lee, W. C., "The EL-DORA/ASTRAIA airborne Doppler weather radar: results from recent field tests," *IEEE Transactions on Aerospace and Electronic Systems*, vol. 11, no. 10, pp. 34-37, 1996.
- [30] Palomar, D. P., and Verdu, S., "Representation of mutual information via input estimates," *IEEE Transactions on Information Theory*, vol. 53, no. 2, pp. 453-470, 2007.
- [31] Slonim, N., Atwal, G., Tkacik, G., and Bialek, W., "Estimating mutual information and multi-information in large networks", 2005 [Online]. Available: [Http://arxiv.org/abs/cs.IT/052017](http://arxiv.org/abs/cs.IT/052017)
- [32] Steuer, R., Kurths, J., Daub, C. O., Weise, J., and Selbig, J., "The mutual information: Detecting and evaluating dependencies between variables," *Bioinformatics*, vol. 8, suppl. 2, pp. S23-S40, 2002.
- [33] Boche, H., and Monich, U. J., "Analytic properties of downsampling for bandlimited signals," *IEEE International Conference on Acoustics, Speech and Signal Processing (ICASSP)*, pp. 5008-5012, 2019.
- [34] Boche, H., and Monich, U. J., "Downsampling of Bounded Bandlimited Signals and the Bandlimited Interpolation: Analytic Properties and Computability," *IEEE Transactions on Signal Processing*, vol. 67, no. 24, pp. 6424-6439, 2019.
- [35] Bergin, J. S., Techau, P. M., Carlos, J. D. Don., and Guerci, J. R., "Radar waveform optimization for colored noise mitigation," *IEEE International Radar Conference*, pp. 149-154, 2005.
- [36] Li, J., Guerci, J. R., and Xu, L., "Signal waveforms optimal-under-restriction design for active sensing," *IEEE Signal Process. Letters*, vol. 13, no. 9, pp. 565-568, 2006.
- [37] Li, J., Stoica, P., and Wang, Z., "Doubly constrained robust Capon beamformer," *IEEE Transactions on Signal Processing*, vol. 52, no. 9, pp. 2407-2423, 2004.
- [38] Stoica, P., He, H., and Li, J., "New algorithms for designing unimodular sequences with good correlation properties," *IEEE Transactions on Signal Processing*, vol. 57, no. 4, pp. 1415-1424, 2009.
- [39] Goodman, N. R., "Statistical analysis based on a certain multivariate complex Gaussian distribution (An Introduction)," *The Annals of Mathematical Statistics*, vol. 34, no. 1, pp. 152-177, 1964.
- [40] Schleher, D. C., "Radar detection in Weibull clutter," *IEEE Transactions on Aerospace and Electronic Systems*, vol. AES-12, no. 6, pp. 736-743, 1976.
- [41] Sekine, M., Ohtani, S., Musha, T., Irabu, T., Kiuchi, E., Hagsisawa, T., and Tomita, Y., "Weibull distributed ground clutter," *IEEE Transactions on Aerospace and Electronic Systems*, vol. AES-17, no. 4, pp. 596-598, 1981.



**Huaping Xu** received her B.S. degree in electronic engineering and Ph.D. degree in communication and information system from Beihang University in 1998 and 2003, respectively. She is currently a Professor with the School of Electronic and Information Engineering, Beihang University.

Her current research interests include synthetic aperture radar (SAR) interferometry, differential SAR interferometry, image processing and radar waveform design. She has now published more than 100 journal and conference papers, and a research

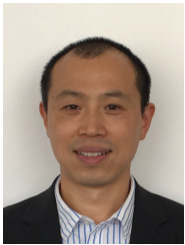
monograph about signal processing.



**Chunsheng Li** received the Ph.D. degree in signal and information processing from Beihang University, Beijing, China, in 1998. Since 2005, he was a Professor with the School of Electronics and Information Engineering, Beihang University. He has authored more than 100 journal and conference papers and four books. His research interests include analysis and simulation of SAR satellite, high-resolution image formation, and multimodal remote sensing data fusion.



**Jiawei Zhang** received the B.S. and M.S. degrees in electronic engineering from Yanshan University, Qinhuangdao, China, in 2014 and 2017, respectively. He is currently working towards the Ph.D. degree with the School of Electronic and Information Engineering at Beihang University. His research interests are in radar waveform design and signal processing for synthetic aperture radar.



**Wei Liu** (S'01-M'04-SM'10) received his B.Sc. in 1996 and L.L.B. in 1997, both from Peking University, China, M.Phil. from University of Hong Kong, in 2001, and Ph.D. in 2003 from the School of Electronics and Computer Science, University of Southampton, UK. He later worked as a postdoc at Imperial College London. Since September 2005, he has been with the Department of Electronic and Electrical Engineering, University of Sheffield, UK as a lecturer, and then a senior lecturer. His research interests are in sensor array signal processing, blind

signal processing, multirate signal processing and their various applications. He has now published more than 250 journal and conference papers, three book chapters, and a research monograph about wideband beamforming.

He is a member of the Digital Signal Processing Technical Committee of the IEEE Circuits and Systems Society and the Sensor Array and Multichannel Signal Processing Technical Committee of the IEEE Signal Processing Society (Vice-Chair from 2019). He is currently an Associate Editor for IEEE Trans. on Signal Processing and IEEE Access, and an editorial board member of the Journal Frontiers of Information Technology and Electronic Engineering.



**Shuang Wang** received the B.S in electronic engineering from Tongjing University, Shanghai, China, in 2018. He is currently working towards the M.S. degree with the School of Electronic and Information Engineering at Beihang University. His current research interest is in signal processing for synthetic aperture radar.